Theory of Discrete Vortex Noise

SANFORD S. DAVIS*
NASA Ames Research Center, Moffett Field, Calif.

A solution is obtained for the noise induced by vortex shedding from the trailing edge of a semi-infinite flat plate. The solution for the potential flow is based on a procedure whereby an inner incompressible flow is matched to an outer acoustic field. Acoustic wave fronts are calculated and compared qualitatively with Schlieren photographs of similar flows. The acoustic directivity pattern is obtained, and the extreme sensitivity of this parameter to the incompressible flow near the trailing edge of the plate is investigated.

Nomenclature

a_∞ = freestream speed of sound
A = const used in conformal mapping
$D(\alpha)$ = directivity factor
D/Dt = convective derivative, $(\partial/\partial t)+V_\infty(\partial/\partial x)$
$F(Z)$ = complex potential, $\Phi(X, Y)+i\Psi(X, Y)$
i, j = $(-1)^{1/2}$
k = acoustic wave number, ω/a_∞
k_x = convective wave number, ω/V_∞
l = typical length scale in region A
M = freestream Mach number
p = pressure perturbation
R = polar coordinate, $(X^2+Y^2)^{1/2}$
r_1 = polar coordinate, $(x^2+\beta^2 y^2)^{1/2}$
r = polar coordinate in physical plane, $(x^2+y^2)^{1/2}$
u = perturbation velocity in X-direction
u_R = perturbation velocity in R-direction
v = perturbation velocity in Y-direction
V_∞ = freestream velocity
x = physical coordinate
X = transformed coordinate, x/β^2
X_o = location of point vortex in Z-plane
X' = scaled coordinate
y = physical coordinate
Y = transformed coordinate, y/β
Y' = scaled coordinate
Z = complex number, $X+iY$
α = polar coordinate in physical plane, $\tan^{-1} y/x$
β = Mach number parameter, $(1-M^2)^{1/2}$
Γ = circulation of point vortex
ζ = complex number, $\xi+i\eta$
ζ_o = location of point vortex in ζ-plane
η = coordinate used in conformal mapping
η_o = location of point vortex in ζ-plane
θ = polar coordinate $\tan^{-1} Y/X$
κ = strength of point vortex $(\Gamma/2\pi)$
κ_o = strength per unit length of vortex sheet
λ = wavelength of acoustic disturbance
ξ = coordinate used in conformal mapping
ρ_∞ = freestream density
$\phi(x, y, t)$ = perturbation velocity potential
$\phi_1(x, y)$ = complex amplitude of perturbation velocity potential
$\Phi(X, Y)$ = transformed velocity potential, ϕ_1/β^4
$\Psi(X, Y)$ = stream function
ψ = phase variable
ω = radian frequency

Introduction

THE effect of extended solid surfaces on the propagation of aerodynamic sound has not yet been fully resolved. Complex diffraction effects at edges and corners are known to have important effects on the acoustic field. Only when the surface involved is considered acoustically compact, i.e., its primary dimensions are at most comparable to the acoustic wavelength, does Curle's dipole analysis[1] reflect the true state of affairs. Recently, several papers were written on the effect of non-compact surfaces on aerodynamic noise. The simplest geometry that encompasses the essence of the problem seems to be the semi-infinite half-plane. Thus, in Refs. 2–8, various aspects of the problem of moving and stationary acoustic sources near a half-plane are discussed.

Recently, Crighton[9] and Jones[10] introduced a new element into the half-plane problem. Crighton showed that the intensity of the aerodynamic noise emitted by an unstable vortex sheet behind a semi-infinite flat plate is extremely sensitive to the imposition of a Kutta condition at the trailing edge. In fact, Crighton[9] reports a change in radiated intensity from ${V_\infty}^4$ without a Kutta condition to ${V_\infty}^2$ with the Kutta condition, as well as a significant change in the directivity factor. Jones[10] shows that imposing a Kutta condition on the field induced by a source near a half-plane results in an intense beaming effect along the wake. Unfortunately, these elegant results are not very amenable to direct experimental confirmation because the idealizations introduced to make the mathematics tractable yield flow models that are difficult to realize physically.

A solution is obtained here for the discrete vortex noise emitted by a semi-infinite plate in a uniform flow. The flow is simple enough to yield to mathematical analysis, yet realistic enough to model quite easily in a wind tunnel. The actual flow to be modeled is that induced by an airfoil section with a blunted trailing edge. The blunted trailing edge is a fixed point of separation for the boundary layer, and a regular vortex street is observed in the wake. Figures 1a and 1b (reproduced with permission from Ref. 11) are two schlieren photographs of the extremely regular vortex wake. Also, cylindrical wave fronts centered at the trailing edge are clearly defined. These wave fronts, distorted by the mean flow, are the aeroacoustic effects of the vortex shedding. The length of the acoustic wave is but a small fraction of the airfoil chord, precluding any dipole-type interpretation of the noise. Since the finite chord seems to have little or no effect on the observed acoustic wave motion, a reasonable mathematical model to this flowfield would be a semi-infinite plate in a uniform flow with a trailing vortex sheet.

The flow model studied is shown in Fig. 2. At the trailing edge of the plate, a vortex sheet is shed with frequency ω. The strength of the sheet κ_o is very small with respect to the freestream velocity V_∞. Both ω and κ_o are determined from considerations that are beyond the scope of this paper. The frequency can most likely be related to a Strouhal number based on V_∞ and the wake thickness,[12] and the strength of the vortex sheet can be related to the form drag of the plate. The irrotational flow induced by this vortex sheet is analyzed in three regions. In region A, the flow is unsteady and incompressible. This region extends to a distance of the order of the scale of the unsteadiness $\sim V_\infty/\omega$. Region C is the acoustic field, where the predominant effect is a propagating acoustic wave.

Presented as Paper 74-90 at the AIAA 12th Aerospace Sciences Meeting, Washington, D.C., January 30–February 1, 1974; received February 21, 1974; revision received September 10. 1974.

Index category: Aircraft Noise, Aerodynamics (Including Sonic Boom).

* Research Scientist. Member AIAA.

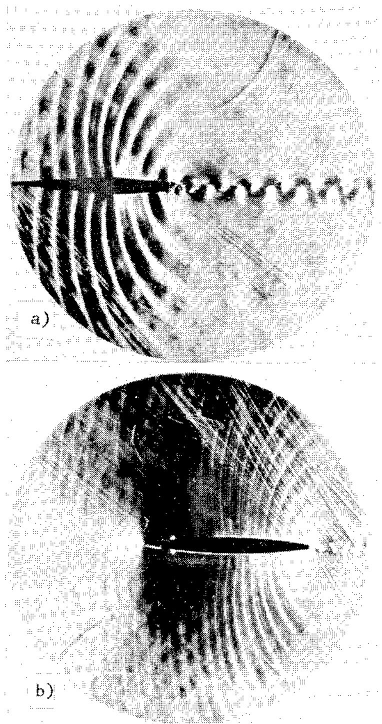

Fig. 1 Schlieren photographs showing discrete vortex noise emitted by a truncated airfoil. a) $f = 6800$ Hz. b) $f = 9520$ Hz.

Solutions obtained in regions A and C are joined in an overlap region—region B in Fig. 2. This method of obtaining a solution is related to singular perturbation techniques, but is most similar to the matching method used by Landau and Lifshitz.[13] The method also gives some insight into the mechanisms of noise generation. It is shown that the extremely complicated incompressible flow is not very important to the acoustic field. Only certain gross properties of the incompressible flow, as reflected by its far-field asymptotic form, are important to the noise field.

Results presented here include acoustic pressure distributions and directivity patterns with and without the imposition of a Kutta condition at the trailing edge. Without the Kutta condition, the familiar cardioid directivity pattern appears and the intensity increases as $V_\infty{}^3$. However, with the Kutta condition a beaming effect along the wake is predicted, and the intensity increases only as V_∞. Either the directivity or the exponent of V_∞ can be used to determine the correct flow experimentally.

Method of Solution

The unsteady vortex sheet induces an irrotational flow in the surrounding medium. Let the velocity be $V_{\text{tot}} = V_\infty + \nabla\phi$, where ϕ is the irrotational perturbation velocity potential. The velocity potential and the perturbation pressure induced by the vortex wake on $y = 0$, $x > 0$ satisfies:

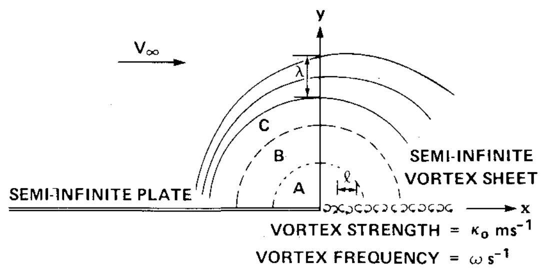

Fig. 2 Idealized flow model used in the analysis. Region A—incompressible flow, region B—transition, region C—acoustic field.

$$\left.\begin{aligned}\nabla^2\phi - (1/a_\infty{}^2)D^2\phi/Dt^2 = 0\\ p = -\rho_\infty(D\phi/Dt)\end{aligned}\right\} \tag{1}$$

where

$$\nabla^2 \equiv \frac{\partial^2}{\partial x^2} + \frac{\partial^2}{\partial y^2}, \qquad \frac{D}{Dt} \equiv \frac{\partial}{\partial t} + V_\infty \frac{\partial}{\partial x}$$

and ρ_∞ and a_∞ are the freestream density and freestream speed of sound, respectively. On the plate itself, the normal velocity must vanish:

$$\partial\phi/\partial y = 0 \qquad \text{on} \qquad y = 0, x < 0$$

and far away from the plate the perturbation velocity must also vanish. In addition, any wave motion must represent outgoing waves at large distances. Equations (1) can be simplified somewhat by substituting

$$\phi(x, y, t) = \text{real part of } [\phi_1(x, y)\, e^{jkMx/\beta^2}\, e^{j\omega t}] \tag{2}$$

where ϕ_1 is a complex amplitude factor, $j = (-1)^{1/2}$, ω is the (assumed known) frequency of the vortex shedding, M is the Mach number V_∞/a_∞, k is the wave number ω/a_∞, and $\beta^2 = 1 - M^2$. The term ϕ_1 can be shown to satisfy

$$(1-M^2)\,\partial^2\phi_1/\partial x^2 + \partial^2\phi_1/\partial y^2 + k^2/\beta^2\,\phi_1 = 0 \tag{3}$$

along with the boundary condition $\partial\phi_1/\partial y = 0$ on $y = 0$, $x < 0$ and appropriate conditions at infinity. It is convenient to rescale the dependent and independent variables as follows. Let

$$\left.\begin{aligned}X &= x/\beta^2\\ Y &= y/\beta\\ \Phi &= \phi_1/\beta^4\end{aligned}\right\} \tag{4}$$

This is similar to, but not exactly like, the classical Prandtl-Glauert transformation. Substituting Eqs. (4) into the equation for ϕ_1 and into the boundary conditions yields

$$\left.\begin{aligned}\partial^2\Phi/\partial X^2 + \partial^2\Phi/\partial Y^2 + k^2\Phi = 0\\ \partial\Phi/\partial Y = 0 \qquad \text{on} \qquad Y = 0, X < 0\end{aligned}\right\} \tag{5}$$

where Φ vanishes as $R = (X^2 + Y^2)^{1/2}$ approaches infinity, and Φ must represent an outgoing wave at infinity. The Helmholtz Equation and boundary conditions in Eqs. (5) are exactly the problem posed in the diffraction of an incoming wave (acoustic or electrodynamic) by a semi-infinite plane.[14] Certain well-known solutions of this problem are used in the following analysis. The transformed potential may then be related to the original perturbation potential by

$$\phi(x, y, t) = \text{real part of}$$

$$[\beta^4\Phi(x/\beta^2, y/\beta)\, e^{jkMx/\beta^2}\, e^{j\omega t}] \tag{6}$$

The basis for a relatively simple analysis of Eqs. (5) is now described. The potential flow near the edge of the plate changes significantly over a length scale l, that must be associated with the incompressible hydrodynamic flow near the edge. The only length scale that can be formed from the kinematic and geometric configuration (Fig. 2) is the wavelength of the vortex sheet $l = 2\pi V_\infty/\omega$. If this length is used to scale the independent variables X and Y in Eqs. (5), the Helmholtz Equation becomes

$$\partial^2\Phi/\partial X'^2 + \partial^2\Phi/\partial Y'^2 + k^2 l^2 \Phi = 0 \tag{7}$$

where $X' = X/l$, $Y' = Y/l$, and $kl = (\omega/a_\infty) \times (2\pi V_\infty/\omega) = 2\pi M$. If M is not too close to unity, the term involving kl is smaller than the two remaining terms. As a first approximation, one could just as well neglect the term in Eq. (7) involving kl. (Actually, this is equivalent to retaining only the first term in a Taylor series expansion of the full potential ϕ about $kl = 0$.) Thus

$$\phi(x, y, t) = Re_j[\Phi(X, Y)\, e^{j\omega t}] \tag{8†}$$

where

$$\left.\begin{aligned}\partial^2\Phi/\partial X^2 + \partial^2\Phi/\partial Y^2 = 0\\ \partial\Phi/\partial Y = 0 \qquad Y = 0, X < 0\end{aligned}\right\} \tag{9}$$

in the original X, Y coordinate system. Thus, near the edge of the plate, the unsteady, incompressible flow satisfies a Laplace

† Re_j is the real part of the complex variable $A + jB$.

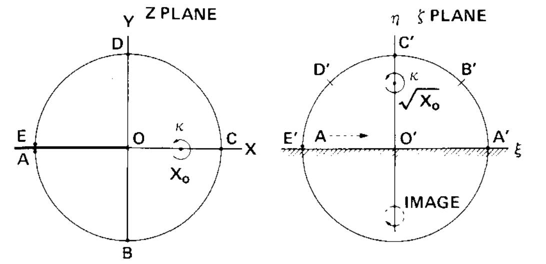

Fig. 3 Conformal mapping for half-plane [transformation: $\zeta = i(Z)^{1/2}$].

Equation. A similar argument that leads essentially to the same result, but for a simpler flowfield, is given by Landau and Lifshitz,[13] and a somewhat more rigorous argument using the singular perturbation approach is given by Crow.[15]

At large distances from the plate edge, a propagating acoustic wave is expected to be the predominant contribution to the perturbation field. In this case, the relevant length scale must be the acoustic wavelength $\lambda = 2\pi/k$. If this length is used to scale the independent variables X, Y in Eqs. (5), the Helmholtz Equation becomes

$$\partial^2\Phi/\partial X'^2 + \partial^2\Phi/\partial Y'^2 + k^2\lambda^2\Phi = 0 \tag{10}$$

where $X' = X/\lambda$ and $Y' = Y/\lambda$. In this case, all terms are of equal importance and the disturbance is governed by the full Helmholtz Equation. Again, for the original coordinate system, Φ must satisfy

$$\left.\begin{aligned} \partial^2\Phi/\partial X^2 + \partial^2\Phi/\partial Y^2 + k^2\Phi &= 0 \\ \partial\Phi/\partial Y = 0 \qquad \text{on} \qquad Y &= 0, X < 0 \end{aligned}\right\} \tag{11}$$

and appropriate conditions at infinity.

The problem, in a sense, is separated into two parts. The burden of satisfying the complicated boundary conditions associated with the vortex motion has been relegated to the inner incompressible flow, and the outer wave region must transmit the acoustic energy associated with the vortex motion. However, this simplification allows Eqs. (11) to be solved only up to a constant multiplicative factor. This factor can be calculated by a matching procedure whereby the limit of the solution to Eqs. (11) as $R \to 0$ is matched to the limit of the solution to Eqs. (9) as $R \to \infty$. This procedure is equivalent to that used in singular perturbation theory, but without explicit reference to the vocabulary of matched asymptotic expansions. Note that Eqs. (11) include a boundary condition that must be satisfied even in the acoustic farfield. This precludes any interpretation of the solution to Eqs. (11) in terms of sources, dipoles, quadrupoles, etc. These multipole concepts are meaningful only at distances far from finite bounded surfaces.

Incompressible Flow Region

In this region (A in Fig. 2), the perturbation potential must satisfy:

$$\left.\begin{aligned} \partial^2\Phi/\partial X^2 + \partial^2\Phi/\partial Y^2 &= 0 \\ \partial\Phi/\partial Y = 0 \qquad \text{on} \qquad Y &= 0, X < 0 \end{aligned}\right\} \tag{12}$$

The solution to Eqs. (12) is obtained by a superposition method similar to that of Burgers.[16] The incompressible flow induced by a single vortex near a half-plane is found most easily by conformal mapping. Let the complex potential $F(Z) = \Phi + i\Psi$‡ in the $Z = X + iY$ plane be mapped into the $\zeta = \xi + i\eta$ plane by the transformation:

$$\zeta = i(Z)^{1/2} \tag{13}$$

As shown in Fig. 3, the half-plane $Y = 0$, $X < 0$ is mapped into the line $\eta = 0$. A vortex of strength $\kappa(\Gamma = 2\pi\kappa)$ at the point $X = X_o$, $Y = 0$ maps into the point $\zeta_o = i(X_o)^{1/2}$ in the ζ-plane. A combination of the vortex, its image with respect to the real axis, and a uniform flow along the real axis satisfies the Laplace equation and the boundary condition. The complex potential is

$$F(\zeta) = A\zeta + i\kappa \log[\zeta - i(X_o)^{1/2}] - i\kappa \log[\zeta + i(X_o)^{1/2}] \tag{14}$$

where A is a real constant. Substitute for ζ from Eq. (13) to obtain the complex potential for a vortex near a half-plane:

$$F(Z) = iA(Z)^{1/2} + i\kappa \log[i(Z)^{1/2} - i(X_o)^{1/2}] - i\kappa \log[i(Z)^{1/2} + i(X_o)^{1/2}] \tag{15}$$

The perturbation velocities, u and v, in the X and Y directions, respectively, can be expressed by means of the complex potential as

$$dF(Z)/dZ = u - iv \tag{16}$$

Differentiating Eq. (15) yields the complex velocity:

$$u - iv = iA/[2(Z)^{1/2}] + i\kappa(X_o)^{1/2}/[(Z)^{1/2}(Z - X_o)] \tag{17}$$

If $|Z| \to 0$, the complex velocity is singular at the edge, and the solution is indeterminate. This singular behavior can be eliminated if a Kutta condition is imposed at the trailing edge. If A is set equal to $2\kappa/(X_o)^{1/2}$, the two terms in Eq. (17) can be combined to yield:

$$u - iv = i\kappa(Z)^{1/2}/[(X_o)^{1/2}(Z - X_o)] \tag{18}$$

Now as $|Z| \to 0$, the complex velocity vanishes and the trailing edge becomes a stagnation point.

A question remains as to whether the complex velocity is correctly given by either Eq. (17) with $A = 0$ (e.g., no Kutta condition) or Eq. (18). The flow is oscillatory, and the frequency of vortex shedding must have an important effect on the imposition of a Kutta condition. If a Kutta condition is imposed, a complicated unsteady viscous flow near the trailing edge is reduced to the imposition of a simple criterion for the location of the stagnation point. Actually, the viscous flow has an associated "relaxation time" over which the flow must respond. If this relaxation time is of the same order as, or greater than, the period associated with the vortex shedding, there would not be enough time for the viscous effects to respond to the full Kutta condition. At very high shedding frequencies, Eq. (17) with $A = 0$ would probably be most correct. On the other hand, at lower shedding frequencies, the Kutta condition [as imposed in Eq. (18)] would most likely be more valid. For the special case when the frequency vanishes (e.g., steady flow), the Kutta condition has been shown to be a good approximation to the actual flow. Further experimentation with these flows is necessary before the true state of affairs can be determined for sure. Both forms of the complex velocity are used here and the acoustic response of the medium is computed for each.

The complex velocity for a continuous vortex sheet can be obtained by superposition. Let the vortex strength per unit length along the wake be κ_o. This vorticity is oscillating at radian frequency ω, and is convected at the freestream velocity V_∞. The vortex strength in a length dX_o of the wake is

$$\kappa = \kappa_o \, dX_o \, Re_j[e^{j\omega(t - X_o/V_\infty)}] \tag{19}$$

The complex velocity when the Kutta condition is applied can be written as an integral over the entire wake as

$$u - iv = -i\kappa_o(Z)^{1/2} \int_o^\infty dX_o \, e^{-jk_x X_o}/[(X_o)^{1/2}(X_o - Z)] \tag{20}$$

where $k_x = \omega/V_\infty$. Note that the time dependence has been suppressed according to the definition of Φ from Eq. (8), and all terms involving j are to be understood as meaning the real part only. (Note that taking the real part with respect to j involves Z as a real constant. Since the velocities u and v are considered explicitly below, the use of two complex variables at this point should not be confusing.) Fortunately, the integral in Eq. (20) is the Stieltjes transform of $e^{-jk_x X_o}/(X_o)^{1/2}$ and is tabulated in the literature. From Erdélyi et al.,[17] the complex velocity is given by

$$u - iv = \pm \pi\kappa_o e^{-jk_x Z} \operatorname{erfc}[\mp i\, e^{j\pi/4}(k_x Z)^{1/2}] \tag{21}$$

‡ The use of i to represent $(-1)^{1/2}$ in this incompressible flow calculation should not be confused with the use of j to represent complex quantities in the preceding section.

where erfc is the Complementary Error Function, and the upper and lower signs are used for $Im\, Z \lessgtr 0$, respectively. This solution satisfies all conditions in Eqs. (12). In the actual flow, the strength of the vortex sheet at the trailing edge does not instantly reach the constant value κ_o as assumed in the calculations. But the potential flow at all points, except right at the trailing edge, depends only on the ultimate vortex strength κ_o, not on the details of the growth of the vorticity.

Consider next the case when no Kutta condition is applied. Let $A = 0$ in Eq. (17), and apply the same procedure used above to obtain the complex velocity:

$$u - iv = \pm \pi\kappa_o[e^{-jk_xZ}\,\mathrm{erfc}\,[\mp i\, e^{j\pi/4}(k_x Z)^{1/2}] \mp i\, e^{-j\pi/4}/(\pi k_x Z)^{1/2}] \tag{22}$$

This solution also satisfies Eqs. (12). These formulas are much too complicated to be used as they stand, but fortunately our interest is only in the effect of these perturbations on the acoustic field. The asymptotic expansion of the Complementary Error Function for large values of its argument is[18]

$$\mathrm{erfc}\,[\mp i\, e^{j\pi/4}(k_x Z)^{1/2}] \sim \pm i\, e^{-j\pi/4}\, e^{jk_xZ}/(\pi k_x Z)^{1/2} \times [1 - j/(2k_x Z)] \tag{23}$$

If this formula is used in Eqs. (21) and (22), the complex velocities become much simpler. The final result for the radial perturbation velocities at large values of $Z = Re^{i\theta}(-\pi \leq \theta \leq \pi)$ is

$$u_R = -(\pi)^{1/2}\kappa_o e^{-j\pi/4} \sin \tfrac{1}{2}\theta/(k_x R)^{1/2} \tag{24}$$

with the Kutta condition and

$$u_R = -(\pi)^{1/2}/2\kappa_o e^{j\pi/4} \sin \tfrac{1}{2}\theta/(k_x R)^{3/2}$$

without the Kutta condition. Although both formulas have a $\sin(\frac{1}{2})\theta$ directivity pattern, application of the Kutta condition imposes a much slower $R^{1/2}$ decay rate rather than the $R^{3/2}$ decay rate when no Kutta condition is applied. These asymptotic forms are still based on incompressible flow theory and can be expected to hold only at distances well within an acoustic wavelength or so from the edge. Region B in Fig. 2 is about the farthest from the plate where Eqs. (24) and (25) can be expected to hold. In the following section, solutions are obtained in the acoustic field which are the compressible flow counterparts of Eqs. (24) and (25).

Acoustic Field

As indicated in Eqs. (11), the perturbation potential must satisfy both the Helmholtz Equation and the semi-infinite plate's boundary condition of no normal flow. Rewriting Eqs. (11) in polar coordinates yields

$$\left.\begin{aligned} &\frac{\partial^2\Phi}{\partial R^2} + \frac{1}{R}\frac{\partial\Phi}{\partial R} + \frac{1}{R^2}\frac{\partial^2\Phi}{\partial\theta^2} + k^2\Phi = 0 \\ &\frac{\partial\Phi}{\partial\theta} = 0 \qquad \text{on} \qquad \theta = \pm\pi \end{aligned}\right\} \tag{26}$$

It can easily be shown by direct substitution that the particular solution

$$\Phi(R,\theta) = \frac{P \sin \frac{1}{2}\theta\, e^{jkR}}{(R)^{1/2}} + \frac{Q \sin \frac{1}{2}\theta\, e^{-jkR}}{(R)^{1/2}} \tag{27}$$

satisfies both the boundary conditions and the partial differential equation. Since only outward bound waves are considered, P must vanish. The acoustic field is determined by Eq. (27) up to an arbitrary constant Q. Now, as kR decreases, the major contribution to the radial velocity is obtained from the derivative of $R^{-1/2}$:

$$u_R \sim \frac{-\frac{1}{2}Q \sin \frac{1}{2}\theta}{R^{3/2}} \qquad \text{as} \qquad kR \to 0 \tag{28}$$

This formula must hold as close in as region B in Fig. 2. But Eq. (25) for the incompressible value of u_R without the Kutta condition must hold as far out as region B. The two equations have exactly the same form except for a multiplicative constant; they are identical if $Q = (\pi)^{1/2}\kappa_o e^{j\pi/4}/k_x^{3/2}$. Hence the potential in the acoustic field, from Eq. (27) is

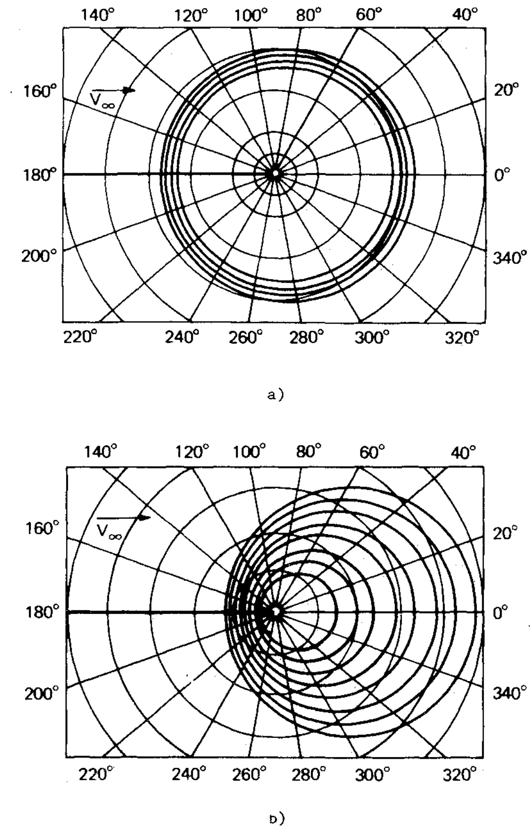

Fig. 4 Wave front pattern in the acoustic field. a) M = 0.10, b) M = 0.60.

$$\Phi = \frac{(\pi)^{1/2}\kappa_o \sin \frac{1}{2}\theta\, e^{-jkR + j\pi/4}}{k_x^{3/2} R^{1/2}} \tag{29}$$

Use of this value of Φ in Eq. (6) gives the acoustic field for a vortex sheet near a semi-infinite flat plate without the Kutta condition. Note that the complicated flow pattern given by Eq. (22) does not affect the acoustic field. Only the gross features of the incompressible flow, as indicated by the asymptotic form in Eq. (25), determine the energy to be emitted as an acoustic disturbance.

The appropriate solution to Eqs. (26) when a Kutta condition is imposed is not as simple as in the preceding case. The only particular solution of Eqs. (26) that can be obtained in the separated form, $\Phi = f(R) \sin \frac{1}{2}\theta$ is that given by Eq. (27). This equation gives a velocity field that decays as $1/R^{3/2}$ in the incompressible region, but a velocity field that decays as $1/R^{1/2}$ in the incompressible region must be obtained. Now consider the complex conjugate of the function given by Crighton[9]:

$$\Phi = Q \exp(-jkR\cos\theta) \int_{(kR)^{1/2}\sin\frac{1}{2}\theta}^{\infty} \exp(-2jt^2)\, dt \tag{30}$$

This function satisfies Eq. (28) and the boundary condition, and has the required outgoing wave behavior as $R \to \infty$. At this point, Eq. (30) bears little resemblance to Eq. (24) with which we wish to match it. However, if the near-field limit is taken as $kR \to 0$, Eq. (30) can be expanded to

$$\Phi = Q\{(\pi)^{1/2}/[2(2)^{1/2}]\, e^{-j\pi/4} - (kR)^{1/2} \sin \tfrac{1}{2}\theta + \ldots\} \qquad \text{as} \qquad kR \to 0 \tag{31}$$

and the major contribution to the radial velocity is given by

$$u_R = -Q/2(k)^{1/2} \sin \tfrac{1}{2}\theta/(R)^{1/2} \qquad \text{as} \qquad kR \to 0 \tag{32}$$

This formula must be valid in region B of Fig. 2. Equations (24) and (32) have the same functional dependence except for constant Q. They would be identical if $Q = 2(\pi)^{1/2}\kappa_o e^{-j\pi/4}/(k_x k)^{1/2}$. Substituting this value of Q into Eq. (30) yields the acoustic field:

$$\Phi = \frac{2(\pi)^{1/2}\kappa_o e^{-j\pi/4}}{(k_x k)^{1/2}} \exp(-jkR\cos\theta)\int_{(kR)^{1/2}\sin\frac{1}{2}\theta}^{\infty} \exp(-2jt^2)\,dt \tag{33}$$

Results

The first quantity examined is the pressure in the acoustic field. From Eqs. (1) and (6), the perturbation pressure can be expressed as

$$p = -\rho_\infty \beta^2[j\omega\Phi(X,Y) + V_\infty(\partial\Phi(X,Y)/\partial X)]\, e^{jkMx/\beta^2 + j\omega t} \tag{34}$$

Consider the case when the Kutta condition was not applied. In this instance Eq. (29) must be used in the formula for the pressure. The farfield pressure ($kR \gg 1$) becomes

$$p = -(\pi)^{1/2} j\rho_\infty V_\infty^{\ 3/2} \frac{\kappa_o(1-M\cos\theta)\sin\frac{1}{2}\theta}{\omega^{1/2}(1-M^2)^{-3/2}(r_1)^{1/2}} e^{j\pi/4}\, e^{j(\omega t - k\psi)} \tag{35}$$

where

$$r_1 = (x^2+\beta^2 y^2)^{1/2}, \qquad \theta = \tan^{-1}\beta y/x$$

and ψ is the phase $(r_1 - Mx)/\beta^2$.

Values of $\psi = \text{const}$ correspond to lines of equal phase for the pressure. These lines are distorted from a circular shape because of the convective effect of the mean flow. Figures 4a and 4b show lines of constant values of ψ for two freestream Mach numbers, 0.1 and 0.6. At the higher speed, the distorting effect is more apparent. A comparison of Figs. 4b and 1b, which correspond to roughly analogous conditions, shows the apparent similarity between the real and calculated wave patterns.

If r and α are polar coordinates in the x, y plane, the directivity factor $D(\alpha)$ is defined by

$$p(r,\alpha,t) = p_o D(\alpha)/(r)^{1/2}\, e^{j\omega t - k\psi} \tag{36}$$

where p_o is some reference pressure. From a comparison of Eqs. (36) and (35),

$$D(\alpha) = \frac{(1-M\cos\theta)\sin\frac{1}{2}\theta}{(\cos^2\alpha + \beta^2\sin^2\alpha)^{1/4}} \tag{37}$$

where $\theta = \tan^{-1}(\beta\tan\alpha)$. The directivity factor is basically a cardioid, but is distorted by the mean flow. Figures 5a and 5b are graphs of $D(\alpha)$ for freestream Mach numbers of 0.1 and 0.6. As shown in the figures, the maximum pressures are directed upstream, and the over-all distribution bears no resemblance to the usual dipole-type directivity attributed to solid surfaces.

The formulas derived above when no Kutta condition is applied are straightforward and easily interpreted. The formulas applicable when the Kutta condition is applied are more complex, and an interpretation of the pressure field by means of a directivity factor is less meaningful. To illustrate the difficulty involved, the pressure perturbation obtained by substituting Eq. (33) into Eq. (34) is

$$p = \frac{-2(\pi)^{1/2}\rho_\infty V_\infty^{\ 1/2} a_\infty^{\ 1/2}\kappa_o}{(1-M^2)^{-1}} \left\{ j(1-M)\, e^{-jkx/\beta^2} \times \int_{(kr_1/\beta^2)^{1/2}\sin\frac{1}{2}\theta}^{\infty} e^{-2jt^2}\,dt + \frac{\frac{1}{2}M\sin\frac{1}{2}\theta\, e^{-jkr_1/\beta^2}}{(kr_1/\beta^2)^{1/2}} \right\} \times e^{-j\pi/4}\, e^{jkMx/\beta^2 + j\omega t} \tag{38}$$

Equation (38) is not in the form of Eq. (36) and no directivity pattern independent of kr_1 exists, no matter how large kr_1 may be. This means that the directivity changes with kr_1, and $D(\alpha, kr_1)$ is proportional to the bracketed term in Eq. (38). Because of its complexity, Eq. (38) is simplified in two angular regions for large values for kr_1. First, if θ is not close to zero, the lower limit of the integral in Eq. (38) is very large. With the asymptotic expansion of the integral in Eq. (38), the formula for pressure becomes

$$p = -\tfrac{1}{2}(\pi)^{1/2}\rho_\infty V_\infty^{\ 1/2} \frac{a_\infty \kappa_o(1-M\cos\theta)}{\omega^{1/2}(1-M^2)^{-3/2}(r_1)^{1/2}} \frac{e^{-j\pi/4}\, e^{j(\omega t - k\psi)}}{\sin\frac{1}{2}\theta} \tag{39}$$

Note that this formula becomes invalid as $\theta \to 0$. Both Eqs. (39) and (35) show a similar decay rate of $r_1^{\ 1/2}$, which is typical of all two-dimensional cylindrical waves. At the other extreme, when $\theta \to 0$, Eq. (38) becomes

$$p = -\frac{1}{(2)^{1/2}}\pi\rho_\infty V_\infty^{\ 1/2} \frac{a_\infty^{\ 1/2}\kappa_o(1-M)}{(1-M^2)^{-1}} \exp j[\omega t - kx(1-M)/\beta^2] \tag{40}$$

The interesting result obtained here is that the acoustic pressure travels out along the wake as a plane wave. As such, it does not decay at large distances from the wing. This curious result is most likely attributable to the singularity associated with the semi-infinite vortex street whose strength is assumed constant at all distances from the plate. At any rate, the pressure perturbation in the acoustic field shows a distinct maximum along the wake when the Kutta condition is imposed. Figure 6 shows probable directivity plots of the pressure distribution for various values of kr. The point on the wake is

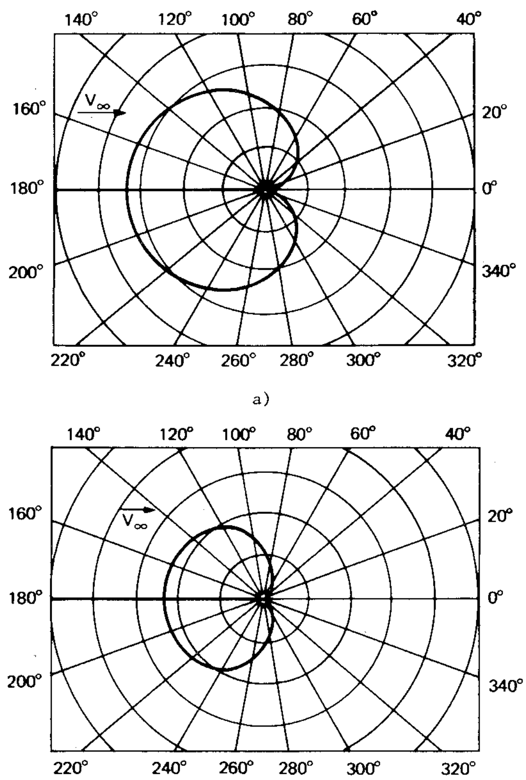

Fig. 5 Directivity pattern in the acoustic field with no Kutta condition applied at the trailing edge. a) $M = 0.10$, b) $M = 0.60$.

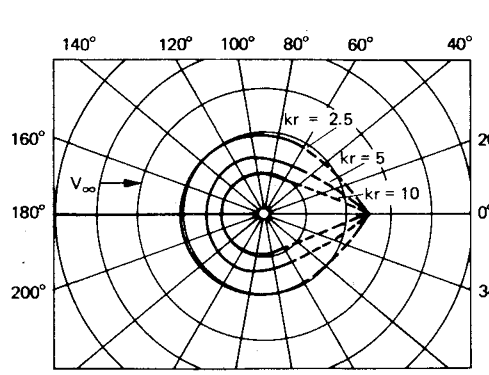

Fig. 6 Directivity pattern in the acoustic field with a Kutta condition at the trailing edge; $M = 0.60$.

known from Eq. (40) and the relative directivity in the upstream direction is calculated from Eq. (39). It seems likely, without going into the computational details of Eq. (38), that the pattern follows the dashed curve used to complete the directivity pattern in Fig. 6. This directivity is unlike those obtained in classical acoustics since there is no "farfield" in the sense that a directivity factor independent of kr can be defined.

The most striking difference in the acoustic field with and without the Kutta condition is shown graphically in Figs. 5 and 6. Another important difference is in the exponent of the freestream velocity dependence. Equations (35) and (38) show that pressure varies as $V_\infty^{3/2}$ (intensity as V_∞^{3}) without the Kutta condition and as $V_\infty^{1/2}$ (intensity as V_∞) with the Kutta condition. In an experimental determination of the true condition to be imposed (this seems to be the only way to decide), either the directivity pattern or the velocity index criterion could be used.

Conclusions

The preceding calculations have shown how a reasonably simple mathematical model can be used to model a realistic aeroacoustic flowfield. During the analysis, the role of the incompressible flow vis à vis the acoustic field was investigated, and it was shown that only certain gross properties of the incompressible flow could affect the acoustic field. The effect of applying a Kutta condition at the trailing edge of the plate was examined, and significant changes were shown in the acoustic field. This result seems to indicate that the entire potential flowfield is very sensitive to conditions at the trailing edge. This behavior is well worth further investigation, for it may be the best region in the entire flowfield for inserting active noise-control devices (e.g., suction and blowing devices as used in high lift applications). It was also shown that the dipole-type directivity pattern, usually associated with the presence of rigid bodies, is not necessarily applicable in the case of large, noncompact surfaces.

References

[1] Curle, N., "The Influence of Solid Boundaries Upon Aerodynamic Sound," *Proceedings of the Royal Society*, Ser. A, Vol. 231, Sept. 1955, pp. 505–514.

[2] Ffowcs Williams, J. E. and Hall, L. H., "Aerodynamic Sound Generation by Turbulent Flow in the Vicinity of a Scattering Half Plane," *Journal of Fluid Mechanics*, Vol. 40, March 1970, pp. 657–670.

[3] Crighton, D. G. and Leppington, F. G., "Scattering of Aerodynamic Noise," *Journal of Fluid Mechanics*, Vol. 43, Oct. 1970, pp. 721–736.

[4] Crighton, D. G. and Leppington, F. G., "On the Scattering of Aerodynamic Noise," *Journal of Fluid Mechanics*, Vol. 46, April 1971, pp. 577–597.

[5] Cooke, J. C., "Notes on the Diffraction of Sound," C.P. 1192, Jan. 1970, Aeronautical Research Council, London.

[6] Chase, D. M., "Sound Radiated by Turbulent Flow Off a Rigid Half-Plane as Obtained from a Wave-number Spectrum of Hydrodynamic Pressure," *Journal of the Acoustical Society of America*, Vol. 52, Sept. 1972, pp. 1011–1023.

[7] Levine, H., "Diffraction Radiation," Papers on Novel Aerodynamic Noise Source Mechanisms at Low Jet Speeds, C.P. 1195, May 1971, Aeronautical Research Council, London.

[8] Crighton, D. G., "Radiation from Vortex Filament Motion Near a Half Plane," *Journal of Fluid Mechanics*, Vol. 51, Jan. 1972, pp. 357–362.

[9] Crighton, D. G., "Radiation Properties of the Semi-Infinite Vortex Sheet," Papers on Novel Aerodynamic Noise Source Mechanisms at Low Jet Speeds, C.P. 1195, May 1971, Aeronautical Research Council, London.

[10] Jones, D. S., "Aerodynamic Sound Due to a Source Near a Half-Plane," *Journal of Institute Mathematics and Applications*, Vol. 9, Feb. 1972, pp. 114–122.

[11] Lawrence, L. F., Schmidt, S. F., and Looschen, F. W., "A Self-Synchronizing Stroboscopic Schlieren System for the Study of Unsteady Air Flows," TN 2509, Oct. 1951, NACA.

[12] Bauer, A. B., "Vortex Shedding from Thin Flat Plates Parallel to the Free Stream," *Journal of Aerospace Sciences*, Vol. 28, April 1961, pp. 340–341.

[13] Landau, L. D. and Lifshitz, E. M., *Fluid Mechanics*, Addison-Wesley, Reading, Mass., 1959, pp. 279–284.

[14] Jones, D. S., *The Theory of Electromagnetism*, Chap. 9, Pergamon Press, Oxford, 1964.

[15] Crow, S. C., "Aerodynamic Sound Emission as a Singular Perturbation Problem," *Studies in Applied Mathematics*, Vol. XLIX, March 1970, pp. 21–44.

[16] Von Kármán, Th. and Burgers, J. M., "General Aerodynamic Theory, Perfect Fluids," in *Aerodynamic Theory*, edited by W. F. Durand, Vol. II, Div. E, Chap. V, 1935.

[17] Erdélyi, A., ed., *Tables of Integral Transforms*, Vol. II, McGraw-Hill, New York, 1954, p. 217, formulas (15) and (16).

[18] Abramowitz, M. and Stegun, I. A., eds., *Handbook of Mathematical Functions*, NBS Applied Math. Ser. 55, U.S. Govt. Printing Office, Washington, D.C., 1964, pp. 297–298.